

Crystal growth and characterization of semiorganic nonlinear optical material: sodium *p*-nitrophenolate dihydrate

S. Brahadeeswaran,^a V. Venkataramanan,^{at} J. N. Sherwood^b and H. L. Bhat^{†**}

^aDepartment of Physics, Indian Institute of Science, Bangalore 560 012, India

^bDepartment of Pure and Applied Chemistry, University of Strathclyde, Glasgow, Scotland, UK G1 1XL

Sodium *p*-nitrophenolate dihydrate (NPNa) is a new semiorganic nonlinear optical crystal. It has a d_{eff} of about 1.2 times that of potassium titanyl phosphate. Large single crystals of NPNa were grown from water and methanol solutions by isothermal solvent evaporation. The morphology of the grown crystals was indexed. The defect content of the methanol grown crystals was evaluated by chemical etching and synchrotron topography. The section topography carried out on a large uncut crystal revealed a considerable reduction in the defect density away from the seed. The improved optical transmission of NPNa crystals was achieved by purifying the starting materials. The mechanical hardness of the NPNa crystals in the 010 plane was evaluated by Vickers and Knoop indentations.

Introduction

Extensive research in the last decade has shown that organic compounds often possess a higher degree of optical nonlinearity than their inorganic counterparts. Some of the advantages of organic materials include inherently high nonlinearity, the ease of varied synthesis, scope for altering the properties by functional substitutions, high damage resistance, *etc.* The quadratic hyperpolarizability in these molecular materials can be written as eqn. (1),

$$\beta = \beta_{\text{add}} + \beta_{\text{ct}} \quad (1)$$

where β_{add} is the additive term resulting from substitution-induced charge asymmetry and β_{ct} , often the dominating factor, is the charge transfer related term [eqn. (2)]¹

$$\beta_{\text{ct}} = \frac{3e^2h^2}{2m} \frac{W}{(W^2 - 2h\omega)^2 - (W^2 - h\Omega)^2} f\Delta\mu \quad (2)$$

where e and m are the electronic charge and mass, $h\omega$ is fundamental photon energy, W is the energy of the optical transition, $\Delta\mu$ is the difference between ground and excited state dipole moments and f is the oscillator strength of transition. In order to optimize β_{ct} , both f and $\Delta\mu$ should be maximized. The high $\Delta\mu$ often results in large optical absorption and high wavelength cut-off. The highly polar nature of these compounds leads to problems in crystal growth and material processing.

A new approach to high efficiency, optical quality, organic based nonlinear optical materials is to consider compounds in which a polarizable organic molecule can be bonded to an inorganic host. An alternative and closely related strategy is to form metal-coordination complexes of highly polarizable organic molecules. These materials are known as semiorganics. In addition to retaining the high optical nonlinearities of the organic molecules, they also possess favourable physical properties. An added advantage is that large single crystals can be grown from low temperature solutions.

Sodium *p*-nitrophenolate dihydrate (abbreviated as NPNa) is a new semiorganic material. It has a d_{eff} of about 1.2 times that of potassium titanyl phosphate (KTP). Minemoto *et al.* have recently reported the linear optical properties, the powder

efficiency for second harmonic generation (SHG) and the crystallographic characterization of the molecule.^{2,3} They have also demonstrated an intracavity frequency doubling of a diode laser pumped Nd:YVO₄ laser.⁴

NPNa is a metal complex of a donor-acceptor substituted aromatic compound [Fig. 1(a)]. It belongs to the orthorhombic crystal class with the space group *Ima2*. The cell parameters are $a=6.892\text{\AA}$, $b=19.692\text{\AA}$ and $c=6.439\text{\AA}$. There are four molecules in the unit cell. Fig. 1(b) is the packing diagram of NPNa as viewed perpendicular to (100). NPNa has a layer structure perpendicular to the crystallographic a axis. The sodium ion is ionically bonded to the nitrophenoxy ion. It also interacts with two oxygens of the solvated water molecules. The charge transfer (CT) axis, defined as that along the donor-acceptor bonds, makes an angle of approximately 80° with the polar axis of the crystal. This alignment is not highly favourable for obtaining the best nonlinear optical coefficients.⁵ However, due to the presence of extensive chains of molecular dipoles, all aligned in the same direction, the functional units contribute additively (as in polymers) to the macroscopic nonlinearity. This arrangement with all molecules aligned parallel is a highly favourable for an optimum electrooptic effect.⁵ Crystals of NPNa are currently being characterized for this property.

The crystal structure of NPNa indicates that the oxygen of

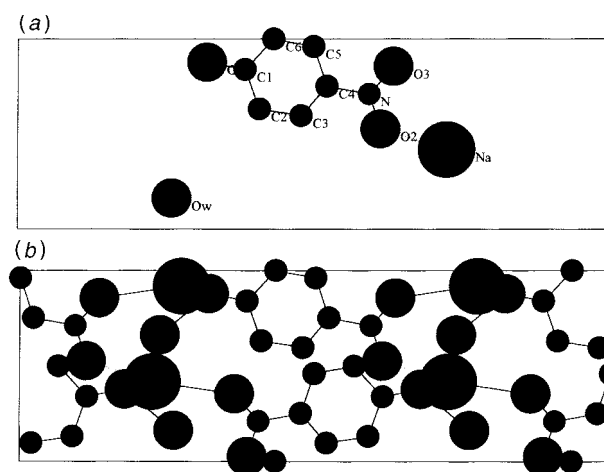


Fig. 1 (a) NPNa molecule, (b) the packing diagram of NPNa as viewed perpendicular to (100) (based on the crystal structure data in ref. 3)

[†] Present address: Center for Advanced Technology, Indore 452 013, India.

^{**} E-mail: hlbhat@physics.iisc.ernet.in

water of crystallization, Ow is hydrogen bonded to the phenolate oxygen O1. These infinitely extending hydrogen bond chains form a network in the *bc* plane. The presence of extensive intermolecular and intramolecular hydrogen bonds, in two almost perpendicular directions, leads to three-dimensional bonding. Because of this the NPNa molecules are expected to show a reasonably high mechanical hardness and no facile cleavage plane. This also influences the development of bulkier habits during crystal growth. The existence of polymeric character (improved optical nonlinearity) and three dimensional bonding network (improved physical properties) are typical of the strategies targeted in engineering semiorganic molecules for nonlinear optical applications. This contribution highlights our experiments and the results of crystal growth from various solvents, morphology, defect characterization by chemical etching and synchrotron topography, optical transmission and mechanical hardness.

Experimental

NPNa was prepared by dissolving nitrophenol in water containing one equivalent of sodium hydroxide. The precipitate was washed and purified by recrystallization from water. The solubility was measured as a function of temperature in the range 25–60 °C. Solutions were prepared in jacketed vessels which were thermostatically controlled (± 0.01 °C). The solution and excess of solute were stirred with magnetic stirring and equilibrated for 8 h before samples were drawn. The solubility was measured gravimetrically.

Single crystals were grown in a solution growth apparatus, the details of which are discussed elsewhere.⁶ The temperature control accuracy was ± 0.02 °C. Evaporation rates were controlled with suitable openings. The morphology of the NPNa crystals grown under various conditions was indexed by measuring interfacial angles of the habit planes using contact and optical goniometers. Thermal analyses were carried out using a Shimadzu DT-40, simultaneous DTA-TG thermal analyser. The heating rate was kept constant for all the runs at 10 °C min⁻¹ and the experiments were conducted in air.

Projection and section topography of NPNa were carried out with synchrotron white beam. Topographs were recorded at Station 7.6 of the synchrotron radiation source at the Daresbury Laboratory (UK). Samples for recording projection topographs were prepared by sectioning the as-grown crystals with a solvent saw. They were further thinned to about 500 μ m on a solvent soaked tissue paper. At this thickness, the product of the mass absorption coefficient (μ) and the thickness of the sample (t), μt is approximately equal to 1, which is optimal for producing kinematic diffraction images.⁷ Section topography on NPNa was performed with a large uncut crystal, grown on a carefully selected seed. The diffraction condition was chosen to give the best contrast images. The topographs were recorded on Ilford L4 nuclear plates. In order to eliminate radiation damage to the sample, undesired long wavelengths of the synchrotron radiation were attenuated with a 3 mm aluminium sheet.

Optical transmission of NPNa was recorded in the 400–2000 nm region, using a Hitachi model 330 spectrophotometer. A 3 mm (010) plate, cut and polished with alumina dispersed in ethylene glycol was used. No anti-reflection coatings were provided. Both Vickers and Knoop hardnesses of NPNa crystals were evaluated in the (010) plane using a Leitz RZD-DO microindenter.

Results and Discussion

Crystal growth

The microanalysis of the synthesized NPNa (Table 1) revealed a good agreement with the calculated values. NPNa has a good solubility in water. Hence we attempted to grow it from

Table 1 Microanalysis of sodium *p*-nitrophenolate dihydrate

	Na(C ₆ H ₄ NO ₃) ₂ H ₂ O		
	C(%)	H(%)	N(%)
computed	36.50	4.10	7.10
experimental	36.47	4.02	6.99

aqueous solution. We could obtain large rod like crystals (up to 4.5 × 2.5 × 1 cm³) in about 3 days. However, these crystals lost their transparency within about 30 minutes of being removed from the mother solution. The optical quality of these water grown crystals could be preserved by immersing them in organic fluids. However, this seriously affects their handling for characterization and device fabrication.

Alternative solvents in which the crystals grown would retain their transparency were explored. Table 2 presents the effect of various solvents on the growth forms of NPNa. The solubilities given are at 30 °C. As can be seen from Table 2, methanol leads to a high solubility and also yields crystals which are transparent and bulky. Hence methanol was chosen as the solvent for detailed crystal growth experiments. The solubility of NPNa in MeOH was evaluated (Fig. 2). Seed crystals of high quality could be developed from the saturated methanol solution by evaporation at room temperature. The seed crystals were optically clear with a bipyramidal morphology. Subsequently large crystals were grown by the controlled evaporation of a saturated solution at 45 °C. The thermostated solution was continuously stirred by accelerated reversible rotation of the seed during growth. The rotation rate was kept low to avoid the formation of localized concentration gradients, whilst ensuring a fair mixing of the solution. The evaporation rates were regulated by suitable openings. Crystals as large as 2.2 × 1.7 × 1.6 cm³ were grown in about two weeks. Fig. 3 shows typical NPNa crystals grown from MeOH solutions. These crystals are fairly nonhygroscopic and retain their transparency.

Initially, we attempted to determine the melting point of NPNa by a visual method, using a Keithley 1951 PRT100 Pt thermometer. We could not observe melting by this direct observation. The compound turned red at around 105 °C on dehydration and brownish at 390 °C indicating a decomposition. We then carried out thermogravimetry (TGA) and differential thermal analysis (DTA) on NPNa (Fig. 4). The TGA indicates a mass loss at 90 °C, coinciding with the endothermic DTA peak. This could be attributed to the loss of water of crystallization. The exothermic DTA peak at 325 °C is associated with a severe mass loss, indicating a decomposition. As can be seen in the thermogram, NPNa does not show any phase transition from room temperature till its dehydration.

Morphology

NPNa crystals always exhibit well developed, clear morphologies with sharp edges, unlike some organic crystals which show curvature of some faces and truncated growth along one direction. The crystals grown from methanol by constant evaporation at room temperature showed a bipyramidal morphology. Table 3 gives a list of calculated and measured interplanar angles of the habit faces. The habit mainly consists of {010}, {011} and {110} faces, with {011} and {110} faces dominating over the *b* planes in the development. As a result the crystals have a shape extended in the <010> direction as shown in Fig. 5(a). The relative development of the faces was {011} ≥ {110} > {010}.

Growth from methanol by evaporation at slightly higher temperatures (45 °C) yielded a bulkier habit [Fig. 5(b)] with a greater development of *b* planes. The relative developments

Table 2 Effect of solvents on growth forms of NPNa

solvent	dipole moment/Debye	solubility g per 100 ml	habit	visual quality	
				as grown	after 24 h
dimethylamine	1.01	8.91	plate-like	transparent	opaque
isopropyl alcohol	1.55	0.51	bipyramidal	transparent	transparent
ethanol	1.69	4.39	bipyramidal	transparent	transparent
methanol	1.70	18.70	bipyramidal	transparent	transparent
water	1.85	6.25	plate-like	transparent	opaque
acetone	2.88	0.96	plate-like	transparent	transparent
dimethylformamide	3.82	23.21	needle	transparent	transparent

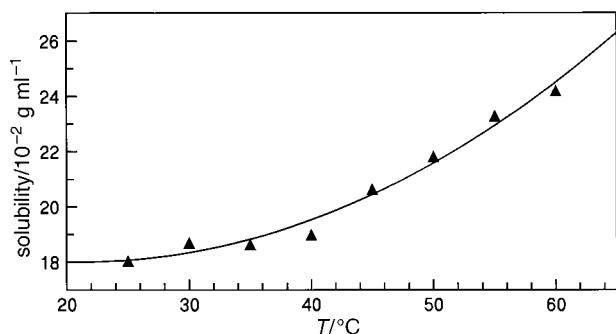


Fig. 2 Solubility curve of NPNa in methanol

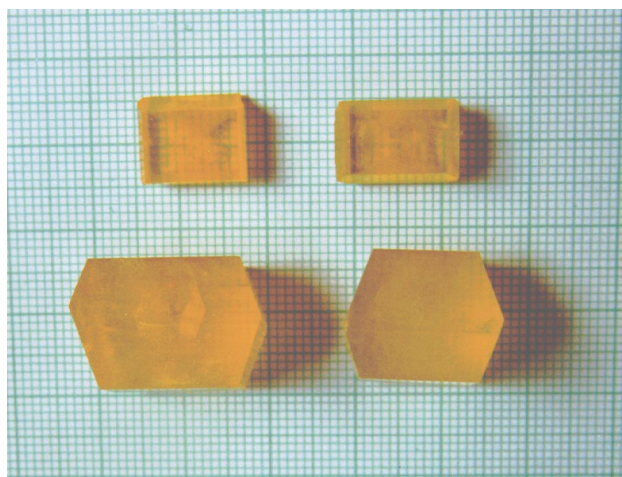


Fig. 3 Photograph of NPNa crystals grown from methanol solution

were $\{010\} > \{011\} > \{110\}$. The growth of $\{011\}$ plane was always unstable, leading to striations. Ultimately, this unstable growth restricted the maximum growable size, by causing spurious surface nucleation.

The morphology of crystals growing under equilibrium conditions can be predicted by a number of methods. One of the simplest, due to Bravais–Friedel and Donnay–Harker (BFDH) relates the habit of the crystals directly to the interplanar spacing, with constraints imposed by the space group.⁸ Accordingly, the faces with largest d_{hkl} will be those dominating the morphology. The most prominent faces, which essentially are the slowest growing, tend to have strong bonding within the layer (or slice). If the crystal face has a pseudosymmetry (due to space group constraints), it will have a slice thickness equal to a submultiple of the interplanar distance. These surfaces will exhibit weak bonding between the slices.^{9,10} The Hartman and Perdok (HP) theory was the first attempt to quantify the crystal morphology in terms of the interaction energy between the crystallizing units.

Since the experimentally observed morphology of NPNa was fairly simple, we considered that a simple BFDH analysis would suffice to predict the morphology. Table 4 lists the slice

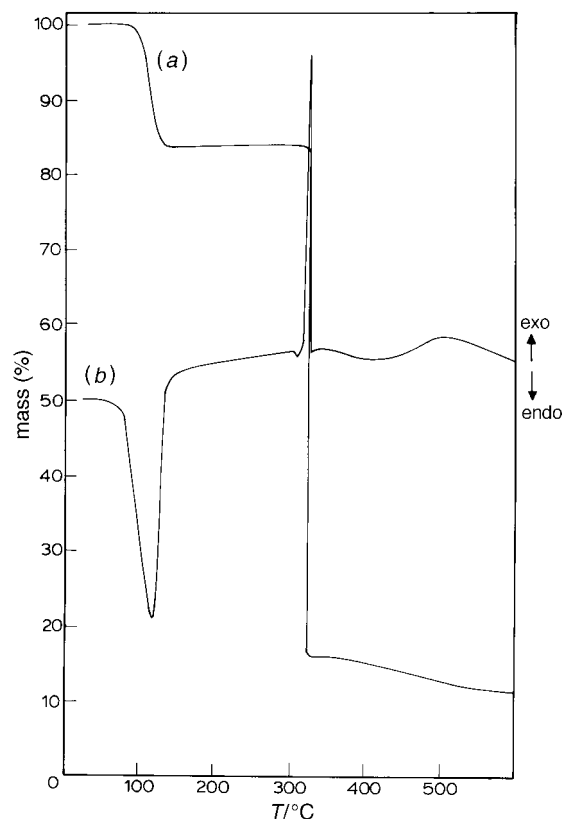


Fig. 4 (a) TGA and (b) DTA of NPNa

Table 3 Calculated and measured interplanar angles ($^{\circ}$) of the habit faces of methanol grown NPNa crystals

angle	calculated	measured
$010 \wedge 100$	70.710	70.0
$010 \wedge 011$	71.893	71.5
$110 \wedge 1\bar{1}0$	38.579	40.0
$011 \wedge 1\bar{1}0$	36.214	36.0

thickness of various faces. As can be seen, there is a good agreement of experimental habit with the predictions from slice thicknesses. For (100) and (010) the presence of pseudosymmetry leads to slice thicknesses equal to one half of their respective interplanar distances. Molecular arrangements on various slices were generated using the computer program ATOMS.¹¹ The slice diagrams indicate a very low bond density for (100) and (001), when compared to all the other morphologically important planes. Fig. 6 shows the bonding in two of the most important morphological planes of NPNa, *viz.*, (010) and (110), and another plane which is absent in the habit, (100). The reticular area is the same in all slice diagrams (100 \AA^2). (010) and (110) have strong bonding in the slices and (100) has a very weak bonding.

The crystals grown from aqueous solution, on the other

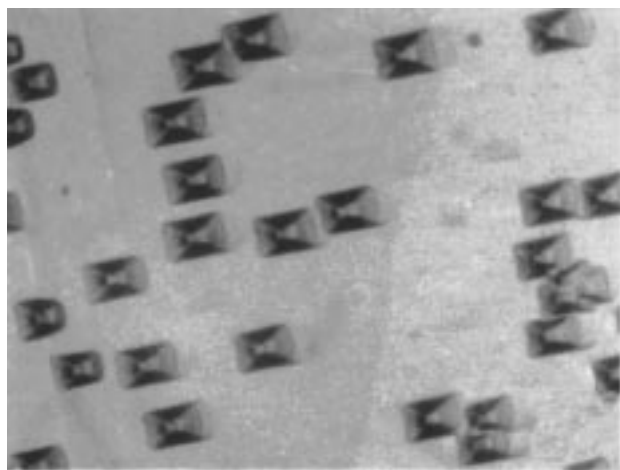


Fig. 7 Etch pits on the (010) plane ($\times 400$)

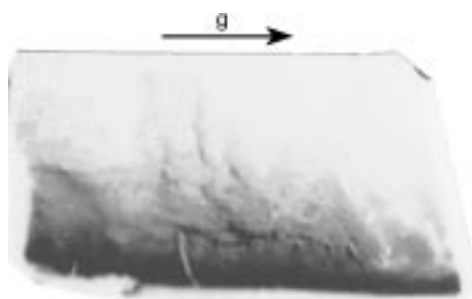


Fig. 8 Synchrotron projection topograph of NPNa; 220 reflection

section, $< 100 \mu\text{m}$) and has the advantage that it could be used to image various parts of a crystal without cutting and polishing. As no mechanical processes (like cutting) are involved in the sample preparation, process-induced defects are eliminated, enabling a true picture of growth induced defects.

The 400 reflection with $F_{400} = 188.9$ and $\theta_B = 26.5$ was used for recording the section topographs of NPNa. At this reflection, the harmonic contamination of the image was small. Fig. 9(a) shows the outline diagram of the crystal topographed. The crystal had visible sectorial inclusions, originating from the seed and fanning out as the crystal grows. Fig. 9(b) shows the series of topographs recorded on various sections as indicated in Fig. 9(a). Section I is close to the center of the crystal incorporating the image of the seed crystal. Sections II and III are those away from the seed, with II being closer to the seed than III. These sections are so chosen as to reveal various stages of the growing crystal. These topographs show some of the common features usually observed in solution grown crystals.¹⁶ These include growth striations (S), growth dislocations (D), growth sector boundaries (B) and solvent inclusions (I). The boundary of the seed is clearly seen in section I. This also has a high relative strain and a large solvent inclusion. The topograph of Section II indicates a considerable reduction in the overall defect density. Growth striations and growth sector boundaries are clearly seen. Further from the seed, slice III shows much improved quality with few defects and lesser inclusions.

Since the section topographs were recorded from a crystal with fully developed morphology, one would expect the image to reveal well defined crystal edges. However, a common feature in all these topographs is the presence of a clearer image of the edges of one pyramidal sector than the sector opposite it. This is a commonly observed problem in topographing molecular crystals.¹⁷ The section topographs reveal

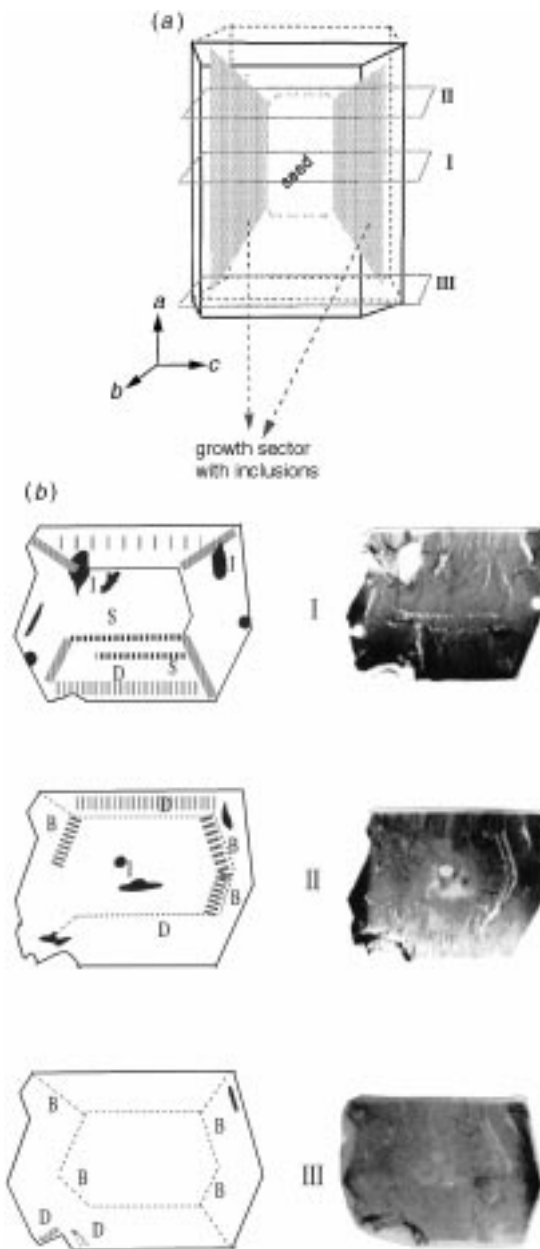


Fig. 9 (a) The outline diagram of the NPNa crystal used in section topography. (b) section topographs of NPNa: (I) a section close to the seed, (II) a section slightly away from the seed and (III) a section further away from the seed, along with their schematics; 400 reflection

that NPNa grows with few defects most of which originate from the seed interface. Projection and section topographs reveal that NPNa has good structural perfection, when compared with other highly polar organic crystals. Feng *et al.* have demonstrated with 4-aminobenzophenone (ABP) crystals that the SHG yields from the crystals with fewer structural imperfections are always higher than those with high defect densities.¹⁸ Hence, for all optical applications, we employ samples cut away from the seed.

Optical transmission. The absorption spectrum recorded for MeOH grown crystal (Fig. 10) shows a lower cut-off at 480 nm, where the transmittance falls by 90%, than that reported by Minemoto *et al.* (515 nm).⁴ We attribute this to the very high purity of the starting materials used for the crystal growth. The solutions used in two growth runs started turning brownish, presumably due to thermal and photochemical degradation. We have always discarded the solutions after every

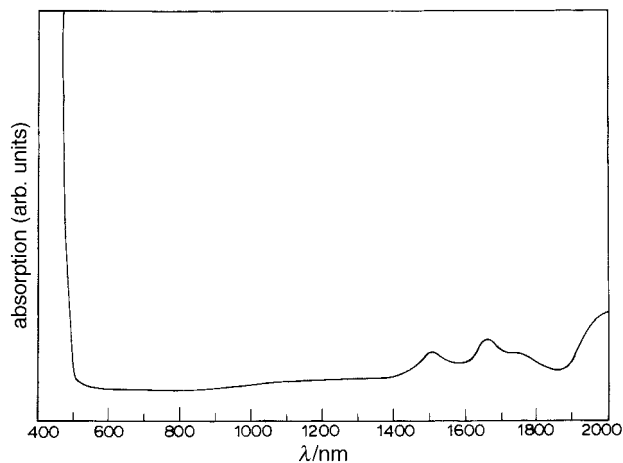


Fig. 10 Absorption spectrum of NPNa from 400–2000 nm

two growth runs. An improved transmission would enable a higher second harmonic throughput. From Fig. 10 it can also be seen that there are three broad bands in the near IR region. While the band at 1580 nm (6329 cm^{-1}) is attributed to the overtone of O–H vibrations of the water molecules the other two, *viz.* 1780 nm (5848 cm^{-1}) and 1860 nm (5376 cm^{-1}), may be attributed to C–H overtones.

Mechanical hardness. An important improvement in the semiorganic crystals over their organic counterparts is their higher mechanical hardness. The typical Vickers hardness value measured for NPNa was 60 at 55 Pa load and the Knoop hardness was 57.2 at 80 Pa. The crystals presented a symmetric indentation even under loads as high as 100 Pa. A load as low as 40 Pa was sufficient to induce cracking in a typical organic crystal like MHBA.¹⁹ The indented crystals were subsequently etched using an acetone–ethanol mixture to assess the dislocation pattern around the indentation. We could obtain a perfect rosette pattern around the mechanical indentation (Fig. 11). The NPNa crystals are quite plastic and are not very brittle. Detailed investigations on the hardness values and the slip systems will be reported elsewhere.

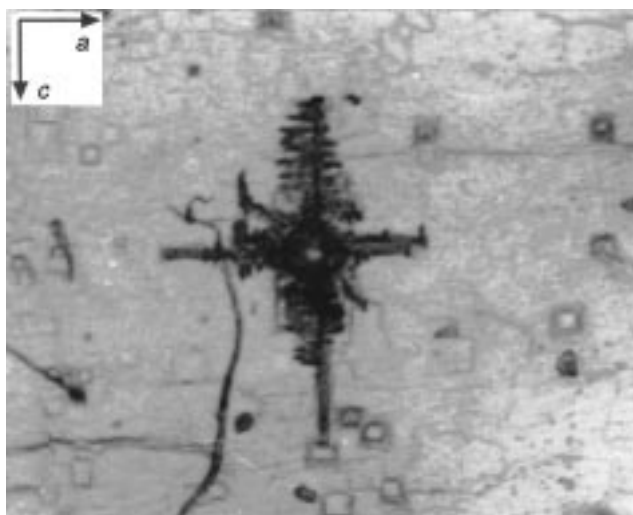


Fig. 11 Rosette pattern around a mechanical indentation in the (010) plane of the NPNa crystal ($\times 400$)

Conclusions

Large single crystals of optically transparent NPNa were grown from methanol solution by isothermal solvent evaporation. These crystals were found to be stable and suitable for optical characterization. The morphology of the crystals grown was indexed. There was good agreement with the experimentally observed morphology and theoretically predicted habit employing BFDH analysis. Defect characterization by chemical etching and topography showed that the crystals grown have low defect contents. Section topography carried out on a large uncut crystal revealed a considerable reduction in the defect density away from the seed. The optical transmission of NPNa crystals were improved by purifying the starting materials. The mechanical hardness of the NPNa crystals in the (010) plane were evaluated by Vickers and Knoop indentations. NPNa crystals were found to be mechanically harder than typical organic crystals.

The synchrotron radiation experiments were carried out at DRAL's Daresbury Laboratory, U.K. We thank the Director and his colleagues for their assistance in this experiment. The help of Dr. G. S. Simpson and Dr. R. Vrelj in the topography experiments is gratefully acknowledged. We would also like to thank Mr. P. Rajeshkumar and Mr. Syed Amanullah for the use of spectrophotometer and TG/DTA thermal analyzer, respectively. One of the authors (V.V) is grateful to the Leverhulme Trust for the award of a Commonwealth Visiting Fellowship.

References

- 1 *Nonlinear optical properties of organic molecules and crystals*, Vol. I, ed. D. S. Chemla and J. Zyss, Academic Press, Florida, USA, 1986.
- 2 H. Minemoto, Y. Ozaki, N. Sonoda and T. Sasaki, *Appl. Phys. Lett.*, 1993, **63**, 3565.
- 3 H. Minemoto, N. Sonoda and K. Miki, *Acta Crystallogr. Sect. C*, 1992, **48**, 737.
- 4 H. Minemoto, Y. Ozaki, N. Sonoda and T. Sasaki, *J. Appl. Phys.*, 1994, **76**, 3975.
- 5 J. Zyss and J. L. Oudar, *Phys. Rev. A*, 1982, **26**, 2028.
- 6 G. Dhanaraj, T. Shripathi and H. L. Bhat, *J. Crystal Growth*, 1991, **113**, 456.
- 7 *X-ray diffraction topography*, B. K. Tanner, Pergamon Press, Oxford, 1976.
- 8 J. D. H. Donnay and D. Harker, *Am. Mineral.*, 1937, **22**, 446.
- 9 P. Hartman and P. Perdok, *Acta Crystallogr.*, 1955, **8**, 521.
- 10 'Modern PBC theory', P. Hartman, in *Morphology of Crystals*, ed. I. Sunagawa, pp. 269–319, Terra Scientific Publishing, Tokyo, 1987.
- 11 ATOMS for Windows, V3.0, Shape Software, Kingport, USA.
- 12 V. Venkataramanan, S. Brahadéeswaran and H. L. Bhat, presented at National Laser Symposium, 10–12 December 1997, PRL, Ahmedabad, India.
- 13 R. T. Bailey, F. R. Cruickshank, D. Pugh and J. N. Sherwood, *J. Optoelectron.*, 1990, **5**, 89.
- 14 P. J. Halfpenny, H. Morrison, R. I. Ristic, E. E. A. Shepherd, J. N. Sherwood, G. S. Simpson and C. S. Yoon, *Proc. R. Soc. Lond. A*, 1993, **440**, 683.
- 15 V. Venkataramanan, S. Uchil and H. L. Bhat, *Bull. Mater. Sci.*, 1994, **17**, 1109.
- 16 B. Yu. Shekunov, E. E. A. Shepherd, J. N. Sherwood and G. S. Simpson, *J. Phys. Chem.*, 1995, **99**, 7130.
- 17 P. J. Halfpenny and J. N. Sherwood, *Phil. Mag. Lett.*, 1990, **62**, 1.
- 18 P. Feng, E. E. A. Shepherd, G. S. Simpson and J. N. Sherwood, personal communication.
- 19 V. Venkataramanan, PhD Thesis, Indian Institute of Science, Bangalore, India, 1994.

Paper 7/05138G; Received 17th July, 1997